J Mater Sci (2008) 43:2929–2934
DOI 10.1007/s10853-007-1798-0

Laser surface melting of electro-metallurgic WC/steel composites

Xianqing You · Chengjun Zhang · Ning Liu · M. P. Huang · J. G. Ma

Received: 22 July 2006 / Accepted: 23 April 2007 / Published online: 3 July 2007
© Springer Science+Business Media, LLC 2007

Abstract Laser surface melting was used to treat electro-metallurgic WC/steel composites. The microstructure and properties of the melted zone were investigated. It was found that a homogenous and fine microstructure was formed in the melted zone. A significant phase precipitated was the herringbone eutectic carbide of Fe_3W_3C. The volume fraction of the eutectics was related to the thermal absorption increasing with the decrease of scanning rate. Preheating was beneficial to form the orientation dendrite structure and to increase the volume fraction of the eutectics. The laser melted surface possessed better microhardness and wear resistance compared to the substrate. The volume fraction of the eutectics played an important role on the wear resistance which increased with the increase of the volume fraction of the eutectics. The wear resistance was mainly depended on the content of the primary WC, as increased with the increase of the content of WC. The improvement of interface bonding, fine eutectic precipitation and structure refinement etc. were regarded as the micro-mechanism of enhancing the surface properties.

Introduction

Tungsten carbide reinforced steel matrix composite (WC/steel composite) as a mold steel has attained a lot of employment in our country due to the abundant resource of tungsten ores. As is well known, the purpose of designing these sorts of particles reinforced metal matrix composites (PMMCs) is to combine the desired properties of the ceramics and metal [1]. The composites usually have a simultaneous high hardness, high strength and a better elastic modulus and reasonable toughness. As a result, the composites can be used to resist wear as well as the coating materials [2–5]. According to the tradition method, powder metallurgy and casting can be used to fabricate the bulk WC/steel composites. However, the disadvantages emerged such as un-compact in powder-metallurgic sample or uneven microstructure in as-cast one. On the basis of the two methods, an electro-slag melting and casting method was developed to improve the materials microstructure [6]. The cast slurry was made by adding the primary WC particles with the diameter of 60 μm into the melting bearing steel of GCr15 (1.0wt%C and 1.5wt%Cr) at about 1,700 °C with the stirring of an electro-magnetic force in electro-slag furnace. Accordingly, the composites obtained can possess better binding of the interface and uniform distribution of WC particles in the steel matrix. After the heat treatment, the composites would have the desired properties finally.

Laser surface melting has been used by many researches as a promising method to improve the properties of the tool steels surface [7–8]. The superior properties obtained by laser surface melting have been exhibited such as a high level of wear, corrosive, erosive and fatigue resistance. The latent practical interest on the superior structure and properties would attract many researchers to carry out the application of laser surface melting to other materials. In addition, the laser surface melting of the WC/steel composites with a higher content of WC has a little report. In this paper we report the laser surface melting of electro-metallurgic WC/steel

X. You (✉) · C. Zhang · N. Liu
Institute of Materials Science and Engineering, Hefei University of Technology, Hefei 230009, China
e-mail: zzxcyj@163.com

M. P. Huang · J. G. Ma
Department of Mechanical and Electrical Engineering, Anhui Architectural Engineering College, Hefei 230022, China

composites, the microstructure and properties of the melted zone were investigated.

Experimental

Electro-metallurgic WC/steel composites of DGW40 and DGW50 were used as the substrate materials of laser surface melting. The content of primary WC added into the DGW40 and DGW50 is 40 and 50wt%, respectively. The material composition was listed in Table 1. The composite were quenched at 1,050 °C and tempered at 450 °C in advance.

Prior to the laser surface melting, the black colloidal graphite was sprayed on the polished surface of specimen to increase the laser absorptivity into the materials. Several specimens of DGW40 and DGW50 were pre-heated at 300 °C by using an electricity resistance equipment. A transverse flow 5.0 kW CO_2 laser was used as laser energy source. Table 2 shows the laser processing parameters.

After laser surface melting, the specimens were mounted, polished and etched by Nital. By using Optical Microscopy (OM) of M-3 and LEO1530 VP Scanning electron Microscopy, the microstructure was analyzed. The phase of laser melted zone was identified by D/max-r B XRD analyzer (target: Cu, 40 kV, 120 mA). The microhardness for cross section was determined by Vichers Microhardness tester.

A block-on-ring apparatus of MM-200 wear tester was used to carry out dry sliding wear tests. The specimen for wear tests was cut into a dimension of 5.5 × 5.5 × 35 mm by wire electrical discharge machining. Figure 2 shows the principle diagram of MM-200 where a bearing steel of GCr15 with the hardness of 62 HRC was used as the wear ring. The load of 196 N was used to perform the wear. The sliding speed is 0.837 m/s, and the wear duration is 20, 30, 40 min, respectively. The specimens were ultrasonically cleaned in acetone prior to and after the wear tests and weighed using an electronic balance.

Volume loss in cubic millimeters per metre of run was calculated as wear rate. Average volume loss of block, for three tests for each alloy, was calculated by the equation [9]

$$\nabla V = G\rho^{-1} \quad (1)$$

where ∇V is the volume loss (mm^3), G the mass loss (g) and ρ the density of composites tested (9.896 g cm^{-3} for DGW40). The specific wear rate (k) was calculated by the simple empirical formula [10]

$$k = HV/sF_n \quad (2)$$

where k is the wear factor or wear rate with the units of $mm^3\ N^{-1}\ m^{-1}$, V the volume loss (mm^3), H the Vicker hardness of the softer material, s the sliding distance (m), F_n the normal force (N).

Results and discussion

Microstructure

Figure 1 shows the laser-melted microstructure of DGW40 without the preheating. It can be seen that the microstructure of the melted zone (MZ) was composed of carbide particles, eutectic and the matrix. And the big and white carbides can be identified as WC particles forming the WC clusters. Furthermore, the volume fraction of herringbone eutectics increases with the decrease of laser scanning rate due to the difference thermal absorption which increases with the decrease of the scanning rate as well. At the same time, the scanning rate was changed from 5 mm/s to 16 mm/s, the depth of melted zone obtained was approximately 0.35 mm and 0.15 mm respectively. Figure 2 shows the XRD diffraction pattern of the melted zone. The diffraction peaks are indexed as WC, Fe_3W_3C, $(Fe, Cr)_7C_3$, martensite and retained austenite(γ-Fe). Compared to the substrate shown in the Fig. 3, it is found that the different phases are formed after laser melting. The appearance of the retained austenite particularly implies that the steel matrix went through re-solidifying. Forming $(Fe, Cr)_7C3$ is possibly caused by the dissolution of Fe into the M_7C_3 in the elevated temperature, and the complex carbide is steadier than the simple one in the steel matrix. The eutectic carbides should be Fe_3W_3C [2, 3]. It can be

Table 2 Parameters of laser surface melting

Number	Laser power (kW)	Laser scan rates (mm/s)	Laser beam diameters (mm)	Scanning tracks
L	2.0	5	6	1
M	2.0	16	6	1

Table 1 Nominal chemical composition of the composites

	C	W	Ti	Si	Cr	Mn	Mo	V	Fe
DGW40	2.66	37.22	0.004	0.012	1.65	0.456	1.13	0.02	Bal.
DGw50	2.71	45.72	0.005	0.11	2.78	0.46	0.31	0.12	Bal.

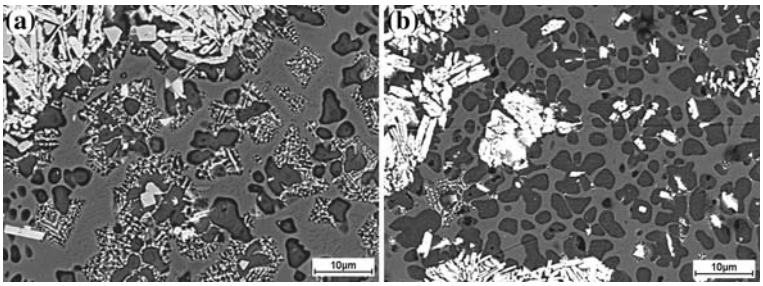

Fig. 1 SEM images of the melted zone of DGW40 without the preheating: (**a**) Processing L; (**b**) Processing M

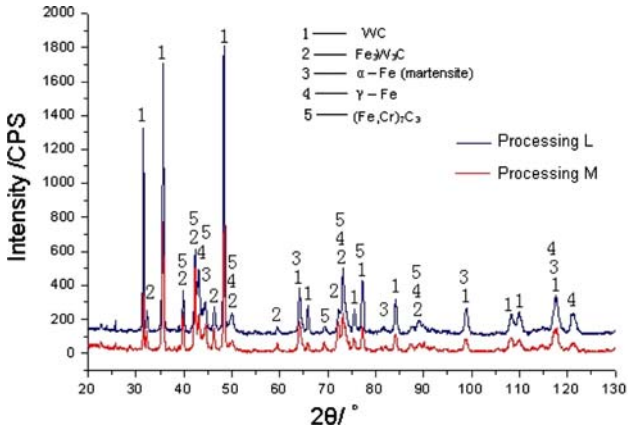

Fig. 2 XRD diagram of the laser melted zone of DGW40 without the preheating

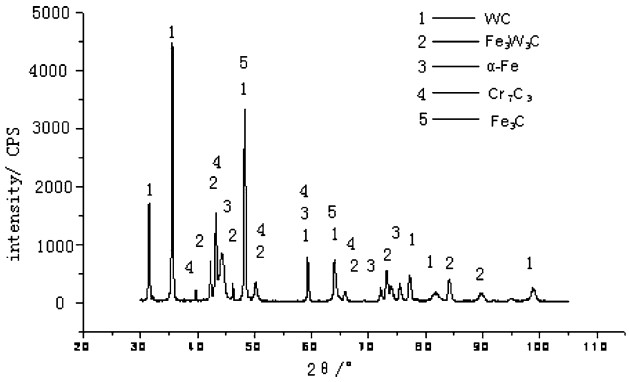

Fig. 3 XRD diagram of DGW40 or DGW50 after the heat treatment

seen from Fig.2 that uniform phases are obtained in the different melted zone, manifesting that the laser interaction to the materials is a thermal conduction process, and the solidified microstructure usually tended to high homogenous owing to the rapid melting and cooling [11–12].

Figure 4 shows the microstructure of the substrate DGW40 and DGW50 after the heat treatment. One can see that the there are two forms of carbides, big white dendritical WC and small carbides, in the steel matrix, and the WC particles cluster is composed of many medium carbides, see Fig. 4c and d. Many regular and irregular carbide particles dispersed in the steel matrix also can be seen. Apparently the fine and dispersed carbide particles are beneficial to reinforce the composites. The XRD analysis as shown in Fig. 3 indicates that the phases of the

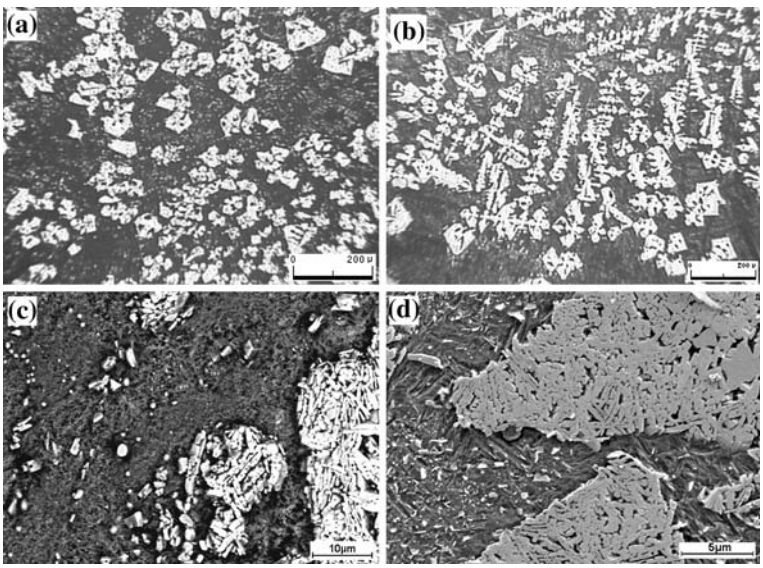

Fig. 4 Microstructure of the composites: (**a**) OM of DGW40; (**b**) OM of DGW50; (**c**) SEM of DGW40; (**d**) SEM of DGW50

composite are composed of α-Fe, WC, Fe_3C, Fe_3W_3C and Cr_7C_3.

Effect of preheating on the microstructure solidified was studied. On the one hand, elevating temperature of preheating would increase the melt depth [13]. On the other hand, it would be beneficial to form the orientation structures [14]. Figure 5 shows OM microstructure of DGW40 with and without preheating after laser surface melting. With the preheating during the melting, the orientation dendrite crystal structure was formed. Figure 6 shows SEM microstructure of laser melted DGW40 with the preheating. Compared to the Fig.1, the volume fraction of eutectic was more, and the dissolved degree of WC clusters increases as well. Furthermore, the primary WC clusters were compacted into bulk WC dendrite. Thus, it implied that the densification of the laser-melted microstructure could be enhanced by elevating the preheating temperature during the melting.

Figure 7 shows the laser melted microstructure of DGW50 with the preheating. As a result, the volume fraction of eutectics precipitated decreases with the increases of the content of WC in electro-metallurgic WC/steel composites. Figure 8 shows the XRD diffraction pattern of the melted zone of DGW40 and DGW50 with the preheating (MZ-DGW40 and MZ-DGW50). The phases of the melted zone consist of WC, Fe_3W_3C, $(Fe, Cr)_7C_3$, martensite and retained austenite. Although the uniform phases were obtained both in the preheating and

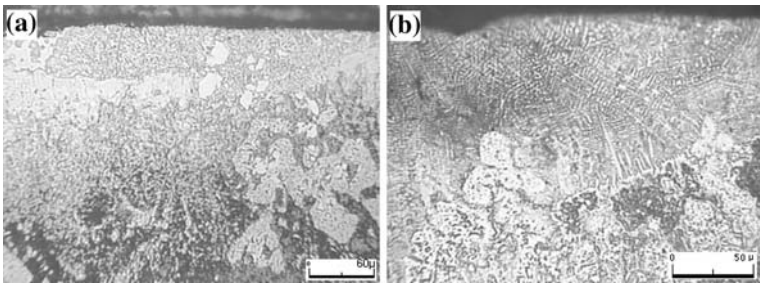

Fig. 5 OM microstructure of the melted zone of DGW40 with the processing L: (**a**) without the preheating; (**b**) with the preheating

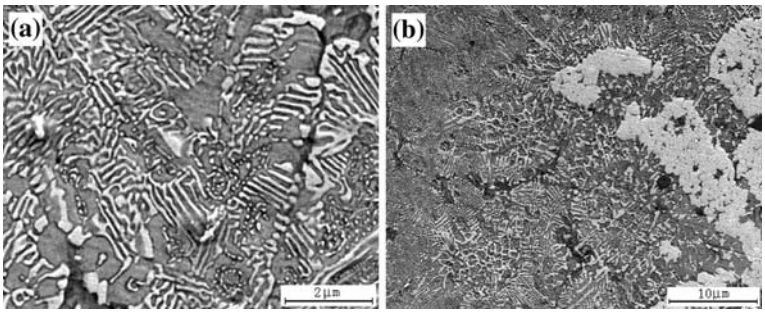

Fig. 6 SEM images of the laser melted zone of DGW40 with the preheating and processing L: (**a**) the eutectics; (**b**) WC and eutectics

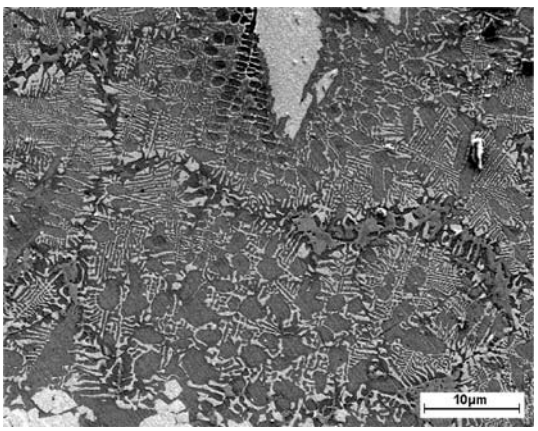

Fig. 7 SEM images of the melted zone of DGW50 with the preheating

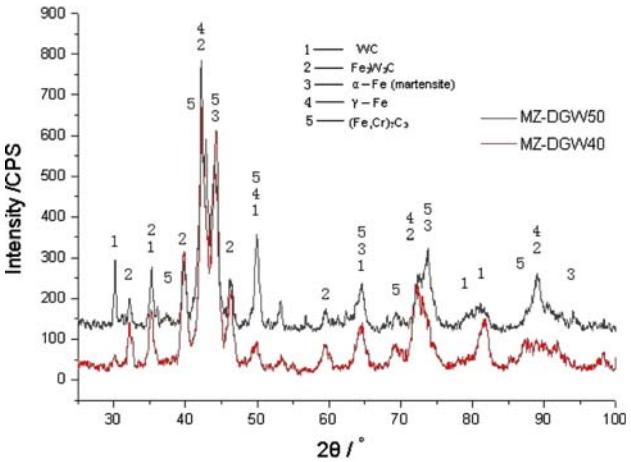

Fig. 8 XRD diagram of the melted zone of the composites with the preheating and processing L

in the un-preheating, the diffraction peaks intensify and breadth are different. The broadened peaks implied that the scale of the solidified grain decreased due to the preheating.

Properties

Figure 9 shows the microhardness profiles along the centre of the melted pool. The micro-hardness of as high as 1300 HV can be obtained in the melted zone while it is approximately 520 HV average in the substrate. The micro-hardness of WC cluster in the melted zone is about 1,500 HV average after testing three times, higher than 1,220 HV of WC cluster in the substrate. Therefore, the surface of the composite can be better hardened by laser melting, and the hardened depth decreases with the increase of laser scanning rate. In addition, the preheating promotes the melt depth, and thus increases the hardened depth as well.

Figure 10 shows the changes of volume loss with the sliding distance for various surfaces. Figure 11 shows the wear coefficient of the various surfaces. The wear resistance of various surfaces under the same content of WC is linked to the volume fraction of the herringbone eutectics. That is to say, the wear volume decreases with the increase of the volume fraction of the herringbone eutectics. At same time, the wear resistance of the melted zone of DGW50 is better than that of DGW40, indicating that the wear resistance was mainly depended on the content of primary WC.

The elevated hardness and excellent wear resistance in the laser melted surface of WC/steel composite are attributed to the improvement of interface bonding, precipitation reinforcement, solid solution of elements and structure refinement. The melting temperature in laser melting is much higher than in the electro-slag melting. The wettability of liquid should increase with the high temperature, improving the interface bonding and making the composites much denser [15]. On the other hand, the reaction layer between the particles and matrix may be formed, which may improve the wettability and may therefore improve the bonding [16]. The situation of interface bonding is considered as the key factor in determining the properties of the composites as is well known. The tighter is the interface bonding, the better the mechanic properties such as wear resistance. In addition, the materials toughness can be improved by structure refinement.

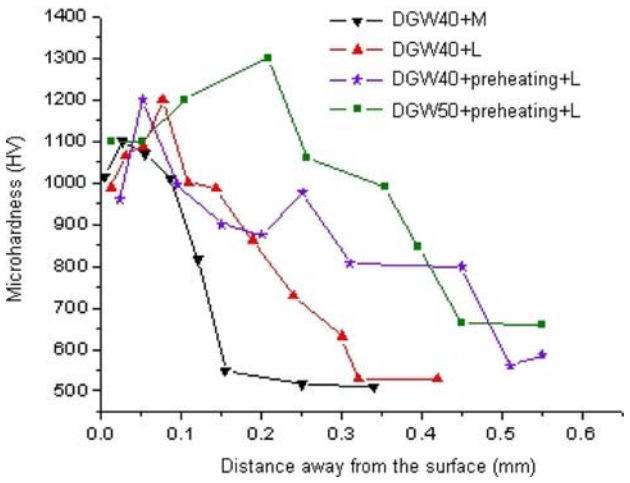

Fig. 9 Microhardness profile along the centre of the melted pool

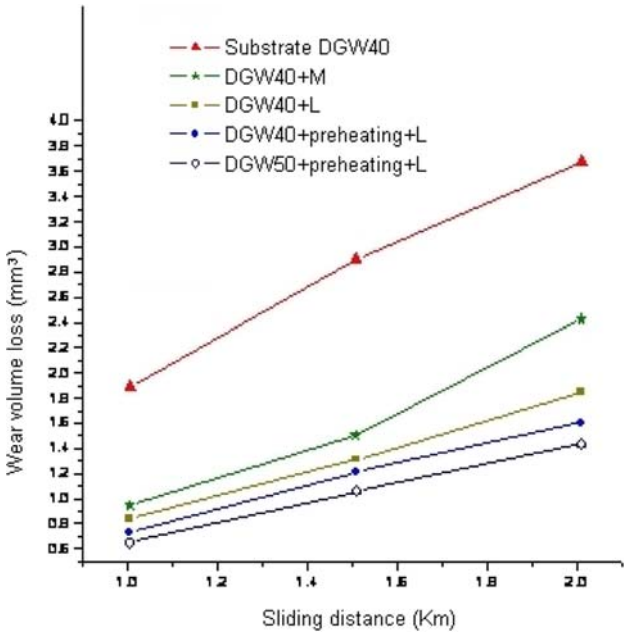

Fig. 10 Volume loss of the wear versus the sliding distance

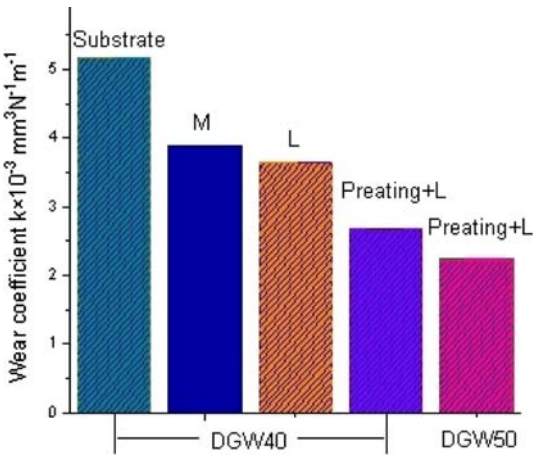

Fig. 11 Wear coefficient of the composites

Conclusion

(1) Uniform phases are formed in different laser melted zone for electro-metallurgic WC/steel composite. The phases consist of WC, Fe_3W_3C, $(Fe, Cr)_7C_3$, martensite and retained austenite(γ-Fe). Compared to the substrate, the surface go through the melting, forming the different phases or microstructures. A particular microstructure is the fine eutectic with the carbide of Fe_3W_3C.

(2) Surface of the composite can possess much better hardness and wear resistance by laser surface melting. The reasons are ascribed to the refined structure, supersaturated solid solution, the precipitated reinforcement and the improved interface bonding between the particles and matrix. The wear resistance increases with the increases of the volume fraction of the herringbone eutectic and the content of primary WC.

(3) Laser scanning rate and the temperature of preheating influence the melt depth and dissolution of carbides in melted zone. The volume fraction of the herringbone eutectics increases with the decreases of the scanning rate. The volume fraction of the herringbone eutectics precipitated with the preheating is more than those obtained without the preheating, and decreases with the increase of content of primary WC.

Acknowledgements We would like to thank the supports of the laboratory center of institute of material science and engineering at Hefei University of Technology. This research was sponsored by the natural science research foundation of department of education of An Hui province in china under Grant NO 2006KG083A.

Reference

1. Hashim J, Looney L, Hashmi MSJ (1999) J Mater Process Technol 92–93:1
2. Kambakas K, Tsakiropoulos P (2005) Mater Sci Eng A 413–414:538
3. Zhao M, Liu A, Guo M et al (2006) Surface Coating Technol 201:1655
4. Zhang G-S, Xing J-D, Gao Y-M (2006) Wear 260:728
5. Panchal PM, Vela T, Robisch T (1990) Fabrication of particulate reinforced metal composites. ASM International, Metals Park, OH, pp 245–260
6. You XQ, Song XF, Ren H (2005) Trans Nonferrous Metal Soc China 15(6):1333
7. Kwok CT, Leong KI, Cheng FT et al (2003) Mat Sci Eng A 357:94
8. Colac R, Vilar R (2004) Mat Sci Eng A 385:123
9. Pirso J, Letunovitš S, Viljus M (2004) Wear 257:259
10. Archard JF (1953) J Appl Phys 24:981
11. Allmen MV (1987) Laser-beam interactions with materiais: physical principles and applications. Springer-Verlag, Berlin, Germany
12. Kac S, Kusinski J (2004) Surface Coating Technol 180:612
13. Shen ZH, Zhang SY, Lu J et al (2001) Optic Laser Technol 33:533
14. Choi J, Choudhuri SK, Mazumder J (2000) J Mat Sci 35:3213
15. Yang Y, Zhu Y, Liu Z et al (2000) Mat Sci Eng 291:171
16. Ocelık V, Matthews D, De Hosson JThM (2005) Surface Coating Technol 197:304